



UNIVERSITY OF LEEDS

This is a repository copy of *Effects of in situ formation of TiB<sub>2</sub> particles on age hardening behavior of Cu-1wt% Ti-1wt% TiB<sub>2</sub>*.

White Rose Research Online URL for this paper:  
<http://eprints.whiterose.ac.uk/81354/>

Version: Accepted Version

---

**Article:**

Sobhani, M, Mirhabibi, A, Arabi, H et al. (1 more author) (2013) Effects of in situ formation of TiB<sub>2</sub> particles on age hardening behavior of Cu-1wt% Ti-1wt% TiB<sub>2</sub>. *Materials Science and Engineering A*, 577. 16 - 22. ISSN 0921-5093

<https://doi.org/10.1016/j.msea.2013.03.063>

---

**Reuse**

Unless indicated otherwise, fulltext items are protected by copyright with all rights reserved. The copyright exception in section 29 of the Copyright, Designs and Patents Act 1988 allows the making of a single copy solely for the purpose of non-commercial research or private study within the limits of fair dealing. The publisher or other rights-holder may allow further reproduction and re-use of this version - refer to the White Rose Research Online record for this item. Where records identify the publisher as the copyright holder, users can verify any specific terms of use on the publisher's website.

**Takedown**

If you consider content in White Rose Research Online to be in breach of UK law, please notify us by emailing [eprints@whiterose.ac.uk](mailto:eprints@whiterose.ac.uk) including the URL of the record and the reason for the withdrawal request.



[eprints@whiterose.ac.uk](mailto:eprints@whiterose.ac.uk)  
<https://eprints.whiterose.ac.uk/>

# Effects of in situ formation of $TiB_2$ particles on age hardening behavior of Cu- 1wt. % Ti- 1wt. % $TiB_2$

Mohsen Sobhani<sup>1)†</sup>, Alireza Mirhabibi<sup>2)</sup>, Hossein Arabi<sup>1)</sup>, R.M.D. Brydson<sup>3)</sup>

<sup>1)</sup>Center of Excellence for high strength alloys technology, School of Metallurgy and Materials Engineering, Iran University of Science and Technology, IUST, Tehran, 16845-118, Iran

<sup>2)</sup>Center of Excellence for Ceramic Materials in Energy and Environmental Applications, IUST, Tehran, 16845-118, Iran

<sup>3)</sup>Institute for Materials Research, University of Leeds, Leeds LS2 9JT, United Kingdom

## Abstract

Age hardenable Cu-1wt. % Ti-1wt. %  $TiB_2$  composite was produced by adding boron powder to Cu-Ti melt.  $TiB_2$  nano particles formed via in situ reaction in the melt. This composite was aged in the temperature range 300-550 °C for 1-25 hrs. The age hardening behavior of composite then compared with that of binary Cu-2 wt. % Ti alloy. The microstructure of the composite was examined with high-resolution transmission electron microscope (HRTEM). The results of this study showed that  $TiB_2$  particles can act as heterogeneous nucleation site for  $\beta'(Cu_4Ti)$  precipitates. Substantial increase in tensile and yield stress of composite (i.e. 63% and 186%) occurred relative to the solution state, after ageing at 450 °C for 10hrs. The maximum strength was associated with precipitation of metastable  $Cu_4Ti$  near to the ultra hard  $TiB_2$  particles within the matrix. However the mechanical properties of composite are comparable with Cu-2 wt. % Ti alloy , the maximum value of the hardness and electrical conductivity of composite (28 %IACS , 258 HV) and Cu-2 wt. % Ti (17% IACS , 264 HV) are obtained when solution treated samples were aged at 450 °C for 10 hrs and 15hrs, respectively.

**Keywords:** Age hardening, Composite,  $TiB_2$ , aging, In situ, Cu-Ti

---

† Corresponding Author , P.O. Box 16845-118, Tehran Iran, FAX: (+9821)77240480 , TEL: (+9821) 77459151, E-mail:m\_sobhani@iust.ac.ir

## 1. Introduction

Copper and copper based alloys are widely used in numerous applications that require high mechanical properties along with good electrical conductivity. Age-hardenable copper-titanium alloys, containing approximately 1–5 wt. % Ti, capable of being a proper substitute for well-known alloys, such as Cu–Be alloys. Formation of ordered metastable  $\beta'$  ( $\text{Cu}_4\text{Ti}$ ) precipitates in Cu-Ti alloys during ageing increases their mechanical and electrical properties [1-3]. The mechanism of precipitation hardening in Cu-Ti binary alloys is a matter of much debate. It has been reported [4] that Cu-Ti alloys with Ti content less than 1 wt. % decompose by nucleation and growth mechanism, while Cu-(2.5-5) wt. % Ti exhibits spinodal decomposition [5].

Nagarjuna and coworkers [3] reported that Cu-Ti alloys having less than 1wt. % Ti are not suitable candidates for age hardening, since the amount of precipitated phase ( $\text{Cu}_4\text{Ti}$ ) achieved by this amount of titanium during aging is very low and approaches to zero in Cu-0.45wt%Ti alloy. On the other hand, it has been reported [6] that by increasing Ti content the electrical conductivity of copper matrix decreases dramatically, as the negative effect of Ti on electrical properties of copper alloys is more than that of other common alloying elements such as Zn, Sn, Ni. Therefore, in order to overcome this problem, some efforts have been made for modifying the precipitation behavior of Cu-Ti alloys via addition of other elements such as Co and Cr [7,8] or by aging in  $\text{D}_2$  and  $\text{H}_2$  atmosphere [1,9].

Among common reinforcing phases for copper matrix, addition of  $\text{TiB}_2$  particles is well known for improving stiffness, hardness and mechanical strength of copper alloys. However, the harmful effect of the dispersed  $\text{TiB}_2$  particles on electrical conductivity of copper is much less than that of other ceramic reinforced particles [10-14]. Although there are some reports about the effect of  $\text{TiB}_2$  particles on copper matrix strengthening via various methods such as powder metallurgy [11], melt mixing [12] and mechanical alloying [13], no reports have been published yet about the effects of in situ formation of  $\text{TiB}_2$  particles on age hardening behavior of Cu-Ti alloy. Therefore, the purpose of this investigation was a comparative study the age hardening behavior, mechanical and electrical properties of Cu-1wt. % Ti-1wt. %  $\text{TiB}_2$  composite and Cu-2wt. % Ti binary alloy.

## 2. Experimental method

The amount of Cu 98%, 1%Ti, 1%TiB<sub>2</sub> composite was considered to be melted in a vacuum induction melting (VIM) furnace. This material is referred as composite in this paper. High purity copper bars (i.e.99.99 %) and titanium plates (99.99%) as well as high purity boron powder (99.98%) with a size range of 0.2-1 mm was used for this purpose. The weight ratio of Ti/B used for producing of this composite was 5.45. In other word, in order to prepare 100 g composite from the following reaction

$Cu + Ti + B = Cu + 1 \text{ wt.} \% Ti + 1 \text{ wt.} \% TiB_2$  it is required to mix 98 g Cu, 1 g Ti and 1 g TiB<sub>2</sub>.

The amount of titanium in TiB<sub>2</sub> is  $1 \text{ g TiB}_2 = (0.31 \text{ g B} + .69 \text{ g Ti})$ .

Therefore, total amount of Ti in composite = free Titanium in matrix+ Ti in TiB<sub>2</sub> thus

The total amount of Ti =  $1 + 0.69 = 1.69 \text{ g}$  and total amount of boron =  $0.31 \text{ g}$ .

Thus, for producing composite with 1 wt. % Ti and 1 wt. % TiB<sub>2</sub>, the weight ratio of Ti/B must be  $m_{Ti}/m_B = 1.69/0.31 = 5.45$ .

In order to prepare the composite encapsulated boron powder into a copper tube (99.99%) was charged into the molten Cu-Ti when the vacuum reached to  $3.5 \times 10^{-2}$  mbar. Melt was held at 1200 °C for 15 min and afterward was cast into a low carbon steel mold fixed with a copper heat sink located at the bottom. In practice the quantitative chemical analysis of titanium by using inductively coupled plasma atomic emission spectroscopy (ICP-AES) was determined 0.94 %. Later the as-cast samples were rolled down to 60% of their thickness at room temperature. Then they were homogenized for 20 hrs at 900 °C in oxygen free molten salt bath, that contained equal weight percent of NaCl and CaCO<sub>3</sub> in order to avoid further oxidation and volatilization of the components. These samples were cooled to ambient temperature in air. After homogenizing the samples, they were subjected to solution-treatment at 900°C in molten salt bath for 1 hour and quenched in water in order to achieve a supersaturated solid solution. The quenched samples were aged in a temperature range of 300-550 °C for 1-25 hrs, and then quenched again in water.

Microhardness of the samples was measured according to ASTM E384-99 standard with 50 g load and tensile tests (cross head speed =  $2 \text{ mm} \cdot \text{min}^{-1}$ ) were conducted at room temperature by cutting strips of the samples according to ASTM E-8 standard. The electrical conductivity of the specimens was measured at room temperature according to ASTM B-193 standard. Scanning electron

microscope (SEM) and high-resolution transmission electron microscope (HRTEM) equipped with electron energy loss spectroscopy (EELS) were used for accurate detection of boron and light elements. In order to compare the effect of  $\text{TiB}_2$  on age hardening, mechanical and electrical properties of the composite, a reference sample with Cu-2 wt. % Ti composition was prepared in such a way that secondary elements in matrix kept constant. All the test performed on the composite were also performed on this reference sample under the same conditions.

### 3. Results and discussion

BS-SEM micrograph in Fig.1. shows the microstructure of 98 wt.% Cu-1wt.% Ti-1wt.%  $\text{TiB}_2$  composite after solidification. Formation of  $\text{TiB}_2$  nano particles within the matrix of the composite can be clearly seen in this figure. Thermodynamically stable  $\text{TiB}_2$  particles can be formed due to chemical reaction between elemental boron and titanium in the molten copper [10-12]. **The  $\text{TiB}_2$  particles that are formed in liquid copper have an irregular shape. The size of  $\text{TiB}_2$  particles is fine but not homogenous. In average the largest size of  $\text{TiB}_2$  particles is about  $1\mu\text{m}$  while the smallest size is less than 100nm. Based on previous research, the  $\text{TiB}_2$  particle size as well as its distribution is affected by many factors including in-situ reaction conditions, cooling rate and elements concentration [10]. According to Cu-B phase diagram, the melting point of boron ( $2092\text{ }^\circ\text{C}$ ) is higher than the melting temperature of the composite, thus boron should chemically dissolved in the molten copper. Accordingly, the boron should gradually react with titanium during dissolution in molten copper. Hence, the boron and titanium solute elements will be absorbed by primarily formed  $\text{TiB}_2$  particles before solidification of copper and result in coarsening and aggregation of smaller  $\text{TiB}_2$  particles according to Gou et al [10]. Therefore, if both titanium and boron elements can be consumed simultaneously take out of the melt, the  $\text{TiB}_2$  nano particles would not have enough time to be easily coarsened.**

**According to solid/liquid interface theories for MMC [15,16], the distribution of  $\text{TiB}_2$  particles is affected by solidification rate, density and wetting angle. In this regards, due to low wettability of  $\text{TiB}_2$  particles by molten copper (i.e. Wetting angle =  $136\text{ }^\circ$ ) [17 ], larger size  $\text{TiB}_2$  particles are**

repelled and redistributed toward the melt-freezing interfaces and finally to the grain boundaries while the smaller size particles are remained inside the grains. Microstructure of composite after the 60% reduction in area and solutionizing was shown in Fig1. b. As shown in this figure due to a relatively good distribution of nano  $TiB_2$  particles within the matrix in comparison to coarse  $TiB_2$  particles, the grain boundaries were pinned by them during re-crystallization. A significant decrease in grain size with the presence of  $TiB_2$  particles after recrystallization shown in Figs. (1.b and 2) which clearly indicate that  $TiB_2$  particles can act as grain refinement in  $\alpha$ -Cu. This is in accordance with other researchers [18] who also reported that the presence of  $TiB_2$  particles in grain boundary can lead to a reduction in grain size and hinder grain growth at high temperature.

Typical TEM images (i.e. bright and dark field) on an as quenched composite with the selected area diffraction pattern (SADP) of  $TiB_2$  particle are shown in Fig.3. This figure shows a large number of tangled dislocations were formed around  $TiB_2$  particles. The difference between the thermal expansions of copper ( $16.6 \times 10^{-6}$  1/K) and  $TiB_2$  particles ( $8.2 \times 10^{-6}$  1/K); leads to development of strain field at the interface between these particles and the copper matrix during quench of the samples from solutionizing temperature to ambient temperature. This thermal strain can cause punching dislocations from the interface of  $TiB_2$  particles out into the matrix. These dislocations and other structural defects can increase the diffusion rate of titanium required for formation  $Cu_4Ti$  and might be appropriate nucleation sites for heterogeneous precipitation of transitional  $\beta'$ ( $Cu_4Ti$ ) phase in the matrix according to Dutkiewicz [19].

Fig.4. shows the typical HRTEM image of the as quenched composite after being re-solutionized at 900 °C for 10 min. HRTEM image together with map of elements via EELS indicates that there is a fair amount of  $TiB_2$  particles formed within the matrix. In addition, this figure shows that titanium concentration increase near the  $TiB_2$  particles. This indicates that  $Cu_4Ti$  is likely precipitated near  $TiB_2$  particles and during the solutionizing for a short time,  $Cu_4Ti$  dissolved near the  $TiB_2$  particles and leading to an increase in titanium concentration at copper/ $TiB_2$  particle interfaces. However, when the composite solutionized at 900 °C for 1hr and aged at 450 °C for 10 hrs a large number of  $\beta'$  ( $Cu_4Ti$ ) precipitates were formed near  $TiB_2$  particles within the matrix. HRTEM micrographs of composite at peak age (maximum hardness) condition (i.e. 10 hrs - 450 °C) with selected area

diffraction (SAD) pattern of  $\beta'$  and FFT pattern of  $\text{TiB}_2$  particle shows in Fig.5. It is clearly evident that a large number of  $\beta'$ ( $\text{Cu}_4\text{Ti}$ ) precipitate was formed in the vicinity of  $\text{TiB}_2$  particle within the matrix. This is an indication of the higher diffusion rate of titanium in the region near the  $\text{TiB}_2$  particles as this region have a high dislocation density as referred to earlier. It should be mentioned that due to heterogeneity of  $\text{TiB}_2$  distribution, the distribution of  $\beta'$  phase was also may be non-homogeneous. This phenomenon confirms that the region having highest dislocation density have great effect in the formation of  $\beta'$  phase. SAD pattern of  $\beta'$  precipitates has been presented in Fig.5 (c). This figure confirms that the particles nucleated near  $\text{TiB}_2$  particles are  $\beta'$ ( $\text{Cu}_4\text{Ti}$ ) as their crystal structure is tetragonal and lattice parameter are  $a=0.584\text{nm}$  and  $C=0.362\text{nm}$ . Unlike the irregular shape of  $\text{TiB}_2$  particles, the  $\text{Cu}_4\text{Ti}$  has a spherical shape with size under  $10\text{nm}$ . Worth mentioning that both needle shape and spherical shape have been reported by other researchers [9, 20, 4] for  $\beta'$  ( $\text{Cu}_4\text{Ti}$ ) precipitates. Fig.5 (b) shows the growth of  $\beta'$  precipitates within the matrix after formation, as the larger particles, may be indicate a nucleation and growth mechanism for formation of  $\beta'$  precipitate according to Borchers [4].

Fig.6. shows the variation of hardness of Cu-1wt. % Ti-1wt. %  $\text{TiB}_2$  composite and Cu-2 wt. % Ti alloy as a function of ageing time. The hardness of the as quenched Cu-1wt. % Ti-1wt. %  $\text{TiB}_2$  (i.e. 115 HV) is higher than that of the as quenched Cu-2 wt. % Ti alloy (i.e. 90 HV). The higher hardness of the composite compares with that of Cu-2 wt. % Ti alloy after quenching was attributed to the presence of  $\text{TiB}_2$  particles, higher dislocation density around  $\text{TiB}_2$  particles and according to Hall-Petch model, to smaller grain size (Fig. 2 and 3).

Ageing curve of the composite in Fig.6 (b) shows that the least hardness was achieved at  $300^\circ\text{C}$  for all ageing time relative to the other temperatures ( $400\text{-}450\text{-}550^\circ\text{C}$ ). At this temperature, hardness decreased at the first two hours of ageing and then raised for further ageing time. Thompson et al [21], reported similar observations for Cu-2.5 wt % Ti alloy. This phenomenon can be explained by considering a) climb and glide of dislocations in the matrix and b) nucleation, coarsening and dissolution of precipitates phase. At  $300^\circ\text{C}$ , before the formation of a considerable amount of  $\beta'$ , climb and glide of punch out dislocation emitted from the presence of  $\text{TiB}_2$  interface within the matrix can be reduced during the ageing process. This leads to relaxation of the interfacial stress and

therefore causes to drop in hardness of the composite in the initial stage of ageing. In addition, the diffusion rate of titanium within the matrix during ageing can be declined by the decrease in dislocation density which cause a delay in precipitation of  $\beta'$ . Thus, one may conclude that 300° C is not enough to provide sufficient energy for higher rates of titanium diffusion that is required for formation of  $\text{Cu}_4\text{Ti}$ . The evidence of the formation of the above mentioned phases by XRD analysis is the subject of another paper which will be published later. Moreover according to Bozic et al [20] as the motion of combined dislocations is strongly dependent on the statistical configuration of the obstacles present in the system, the structural ordering in titanium rich region and disappearance of anti phase boundary in early moments of ageing have resulted in an easy dislocation motion. As a result, the hardness decreases in the first 2 hrs of the ageing. Then with further ageing time, the hardness of the composite can increase due to the formation of metastable precipitation of  $\text{Cu}_4\text{Ti}$  ( $\beta'$ ) in matrix. Nevertheless, more investigations are needed to be performed for clarification of this phenomenon.

Hardness of composite and binary alloy increases with increasing ageing time at 400 °C. However, both of them aren't corresponding to peak hardness even after 25 hrs ageing at this temperature. The volume fraction of  $\beta'$ - $\text{Cu}_4\text{Ti}$  precipitate increases considerably with Ti content as well as ageing time according to lever rule. Therefore the amount of precipitate phase of  $\beta'$  which formed in binary alloy is higher than those for composite sample and hence the hardness of binary alloy is higher than that of the composite.

Variation of hardness with ageing time at 550°C is presented in Fig.6. (a, b). This figure shows that hardness increases in the first two hours of ageing. This is in agreement with the reported work of Datta an Soffa [22] who attributed the increase hardness to formation of ordered meta stable and coherent  $\beta'$ ( $\text{Cu}_4\text{Ti}$ ) phase within the matrix. However, hardness decreases after 2 hrs of ageing at 550 °C. This can be due to polymorphic transformation of  $\beta'$ ( $\text{Cu}_4\text{Ti}$ , tetragonal) to  $\beta$  ( $\text{Cu}_4\text{Ti}$ , orthorhombic) and precipitates growth according to Soffa et al [2]. According to Cu-Ti phase diagram [2], it is indicated that the temperature of 550° C for composite with 1 wt. % Ti is above the solvus line, while this temperature is below the solvus line for binary alloy. Thus, it can be concluded that ageing of composite at this temperature lead to a faster dissolution (over aging) of precipitate phase in

the matrix than binary alloy, and also resulting in reduction in hardness after 2 hrs ageing at this temperature. It can also be seen that the maximum hardness of the composite is lower than that of the binary alloy, which in turn is due to the formation of the lower amount of precipitate phase within the matrix in comparison to binary alloy, as mentioned earlier.

The effective factors on hardness (i.e. dislocation elimination and formation of precipitate), change in such a way that cause a gradual increase in hardness at 450 °C with increasing ageing time. In the absence of TiB<sub>2</sub> particles, the maximum hardness of Cu-2 wt. % Ti alloy (i.e. 264 HV) occurred after 15 hrs while the maximum hardness of composite (i.e. 258 HV) achieved after 10 hrs ageing at 450 °C. The increasing in ageing kinetic in the presence of TiB<sub>2</sub> particles can be attributed to possible nucleation of β' precipitates on the basal plane of TiB<sub>2</sub> and over punch out dislocation as shown in Fig.5 (a). The rate of decrease in hardness after passing the peak value in the composite (i.e. 0.9 HV/hr) is less than that of Cu-2 wt. % Ti alloy (i.e. 1.1 HV/hr). This behavior can be explained by retarding influence of TiB<sub>2</sub> particles on the coarsening of larger number of metastable Cu<sub>4</sub>Ti particles according to Bozic et al [20]. On the other hand, according to a similar research by Cornie et al [23] decrease in hardness value of Cu-2 wt. % Ti alloy after peak age condition can be due to the formation of cellular (discontinuous) precipitates at the grain boundaries, see Fig.7.

Hardness, tensile properties and electrical conductivity of the as cast, as quenched and peak-aged composites were measured and presented in Table.1 together with similar properties of Cu-2 wt.% Ti binary alloy. The results show a considerable increase in electrical conductivity of peak aged (i.e. 28% IACS) composite relative to as cast (8% IACS) and as quenched (15% IACS) condition. As the titanium significantly reduces the electrical conductivity of copper [3], the formation of Cu<sub>4</sub>Ti consumes the titanium in matrix and causes to reduce the electrical resistivity. In other words, the increasing in resistivity due to the increasing volume fraction of Cu<sub>4</sub>Ti precipitate is lower than the decrease in resistivity due to removal of Ti from the matrix [6], therefore resulting in an overall increase in electrical conductivity in peak-aged composite compared with the solution treated one. As shown in this table, the electrical conductivity of the composite at peak aged condition is 65% higher than those of the binary Cu-2 wt.% Ti alloy. This higher electrical conductivity is analyzed by considering the interaction between conductive electron and reinforced particles. In that regard, two

effective factors can be considered in evaluating the electrical conductivity of copper matrix, which are resistivity of particles and scattering surface of conductive electrons. As the electrical resistivity of  $\text{TiB}_2$  particles (i.e.  $6.6\mu\Omega\text{cm}$ ) [24] is lower than  $\text{Cu}_4\text{Ti}$  (i.e.  $38.5\mu\Omega\text{cm}$ )[6] precipitate, it can be concluded that the detrimental effect of  $\text{TiB}_2$  particles on electrical conductivity of copper is lower than  $\text{Cu}_4\text{Ti}$  precipitates. On the other hand, as mentioned previously, the amount of  $\text{Cu}_4\text{Ti}$  precipitate, which is formed in peak-aged condition of the composite, is lower than that of binary alloy. Also these precipitates were preferably nucleated next to the  $\text{TiB}_2$  particles. Hence, the scattering surface of conductive electrons due to formation of  $\text{Cu}_4\text{Ti}$  precipitates in composite did not much rise during ageing process in comparison to binary alloy. Consequently the electrical conductivity of composite increases more than binary alloy during the ageing according to Nordheim's rule [6,3].

Table.1. shows a substantial increase in tensile properties of the sample under peak-aged condition when compared with those of the as quenched sample. The amount of increase in yield and tensile strength of the peak-aged composite sample relative to the as quenched sample are 270 MPa and 228 MPa respectively; while those increases for the Cu-2 wt. % Ti binary alloy are 232 MPa and 197 MPa respectively. Therefore, since the amount of increase in the ultimate and yield strengths of composite during ageing were higher than those of binary Cu-2 wt. % Ti alloy. One may conclude that the mechanism of strain hardening in the composite having both non-shearable  $\text{TiB}_2$  particles and shearable  $\beta'$  ( $\text{Cu}_4\text{Ti}$ ) particles was a difference in the mechanism of strain hardening of Cu-2wt. % Ti alloy without any non-shearable strengthening particles. In other hand in the composite, both shearable and non-shearable particles can slow down dislocation movement leading to high strength. While in Cu-2 wt. % Ti alloy only the shearable  $\beta'$  effect the strengthening of the alloy. This means that consecutive passes of dislocation through these particles decreases, so the required force for movement of dislocation through these particles gradually decreases [3]. The ductility of composite (%EL=21) is slightly less than that of Cu-2wt. % Ti alloy (%EL=24) under peak aged condition. This was attributed to the presence of ultra hard  $\text{TiB}_2$  particles in the matrix of the composite which lowered the dislocation movement hence lowered ductility, nevertheless dimple characteristic of the fracture surface of composite (Fig.8) indicate a ductile mode of fracture in the composite.

#### **4. Conclusions**

1-In Situ formation of  $\text{TiB}_2$  in Cu-1 wt. % Ti-1 wt%  $\text{TiB}_2$  composite makes it possible to access to a favorable combination of high hardness and electrical conductivity after ageing treatment. During the ageing,  $\text{Cu}_4\text{Ti}$  reinforcing particles preferably precipitate near  $\text{TiB}_2$  particles. This is because of the punched out of dislocations around the  $\text{TiB}_2$  particles, which introduces heterogeneous nucleation sites.

2-HRTEM characterization of Cu-1 wt. % Ti-1 wt. %  $\text{TiB}_2$  composite confirm the presence of metastable  $\beta'(\text{Cu}_4\text{Ti})$  precipitate formed near the  $\text{TiB}_2$  particles when aged at 450 °C for 10 hrs.

3-Ductile mode of fracture was observed in Cu-1 wt. % Ti-1 wt. %  $\text{TiB}_2$  composite at peak age condition.

4- The electrical conductivity of the composite increase due to formation metastable precipitates ( $\beta'$ ) in matrix and reach to 28% IACS after 10 hrs aging at 450 °C.

5-The maximum hardness, yield and ultimate tensile strengths of composite (258 HV, 415 MPa, 590 MPa; respectively) are achieved after 10 hrs while the maximum mechanical properties of Cu-2 wt.% Ti (264 HV, 417 MPa , 615 MPa; respectively) achieved after 15 hrs ageing at 450 °C.

#### **Acknowledgment**

The authors are grateful to the professor. R. M. D. Brydson , School of Process, Environmental and Materials Engineering, University of Leeds, for providing a TEM facility in Leeds Electron Microscopy and Spectroscopy Centre. The authors would like to express their gratitude to the Iranian nanotechnology initiative for financially supporting this project.

## References

- [1] S. Semboshi, T. Al-Kassab, R. Gemmab, R. Kirchheim, *Ultramicroscopy*.109 (2009) 593–598.
- [2] W. A. Soffa, D. E. Laughlin, *Prog.Mater. Sci.* 49 (2004) 347–366.
- [3] S. Nagarjuna, M. Srinivas, K. Balasubramanian, D. S. Sarma, *Mater. Sci. Eng. A* 259 (1999) 34–42.
- [4] C. Borchers, *Philos. Mag. A* 79-3 (1999) 537-547.
- [5] I.S. Batra, G. K. Dey, U. D. Kulkarni, S. Banerjee, *Mater. Sci. Eng. A* 360 (2003) 220-227.
- [6] S. Nagarjuna, K. Balasubramanian, D.S. Sarma, *Mater. Sci. Eng. A* 225 (1997) 118-124.
- [7] S. Nagarjuna, K. K. Sharma, I. Sudhakar, D.S. Sarma, *Mater. Sci. Eng. A* 313 (2001) 251–260.
- [8] R. Markandeya, S. Nagarjuna, D. S. Sarma, *Mater. Charact.* 57 (2006) 348–357.
- [9] S. Semboshi, T. Nishida, H. Numakura, T. Al-Kassab, R. Kirchheim. *Metall. Mater. Trans.A.* 42A (2011)2136-2143
- [10] M. Guo, K. Shen, M. Wang, *Acta Mater.* 57 (2009) 4568–4579.
- [11] S. Dallaire, J.-G. Legoux, *Mater. Sci. Eng. A* .183 (1994) 139-144.
- [12] J. H. Kim, J.H. Yun, Y.H. Park , K.M. Choa, I.D. Choi , I.M. Park, *Mater. Sci. Eng. A.* 449–451 (2007) 1018–1021.
- [13] S. J. Dong, Y. Zhou, Y. W. SHI, B. H. Chang, *Metall. Mater. Trans. A.* 33A (2002) 1275-1280.
- [14] P. Yid, D.D.L. Chung, *J. Mater. Sci.*32 (1997)1703-1709.
- [15]D. Shanguan, S Ahuja, DM Stefanescu. *Metall Trans A.*23 (1992) 669-680.
- [16]DM. Stefanescu, BK Dhindaw, SA Kacar, A Moitra. *Metall Trans A.*19 (1988) 2847-2855.
- [17] G. A. Yasinskaya, *Powder Metall. Met.Ceram.* 5-7 (1966) 557-559.
- [18] Z.Y. Ma, S.C. Tjong. *Mater. Sci. Eng. A.* 248 (2000) 70-76.

- [19] J. Dutkiewicz, Metall. Trans. A. 8 (1977) 751-761.
- [20] D. Božić, J. Stašić, J. Ružić, M. Vilotijević, V. Rajković, Mater. Sci. Eng. A 528 (2011) 8139-8144.
- [21] A.W. Thompson, J.C. Williams, Metall. Trans. A. 24 (1984) 931-937.
- [22] A. Datta, W.A. Soffa, Acta Metall. 124 (1976) 987-1001.
- [23] J.R. Cornie, A. Datta, W.A. Soffa, Metall. Trans. A. 4 (1973) 727-733.
- [24] F.W. Vahldiek, J. Alloys Compd. 3(1976) 202-209.

## Figures and Table Captions

**Fig. 1 BS-SEM micrograph of Cu-1wt. %Ti-1wt. %TiB<sub>2</sub> composite after a) solidification b) cold work and solutionized**

**Fig.2 Microstructure of Cu- 2 wt. % Ti after quenching from 900°C**

**Fig. 3. a) Bright field TEM image of tangled dislocations in the vicinity of TiB<sub>2</sub> particles after quenching b) Dark field (c) SAD pattern of TiB<sub>2</sub> particle.**

**The Fig.4 HRTEM image of the re-resolution and quenching Cu-1wt. %Ti-1wt. %TiB<sub>2</sub> with dot point elements maps**

**Fig. 5 HRTEM micrograph of Cu-1wt. % Ti-1wt. % TiB<sub>2</sub> aged at 450 °C for 10hrs (a) β'(Cu<sub>4</sub>Ti) formed near the TiB<sub>2</sub> particle (b) β' growth (c) SAD pattern of β'(Cu<sub>4</sub>Ti) (d) TiB<sub>2</sub> FFT pattern**

**Fig.6. Variation of hardness as a function of ageing time in different temperatures (a) Cu-2 wt. % Ti (b) Cu-1%wtTi-1%wtTiB<sub>2</sub>**

**Fig.7. Microstructure of Cu-2 wt. % Ti binary alloy after 25 hrs aged at 450 °C, shows the formation of cellular type precipitate at grain boundaries**

**Fig.8. Fracture surface of Cu-1 wt. % Ti-1wt. % TiB<sub>2</sub> composite after 10 hrs aged at 450 °C**

**Table.1. Comparison of properties of Cu-1wt. % Ti-1 wt. %TiB<sub>2</sub> composite with that for Cu-2 wt. % Ti**

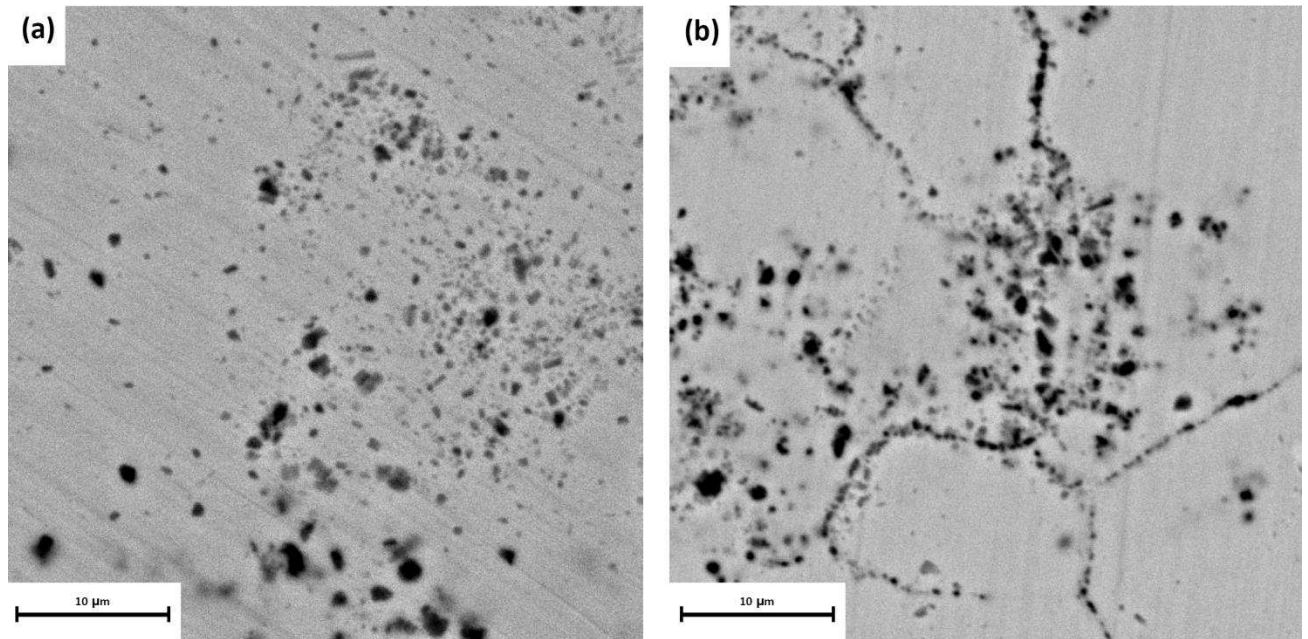


**Fig. 1 BS-SEM micrograph of Cu-1wt. %Ti-1wt. %TiB<sub>2</sub> composite after a) solidification b) cold work and solutionized**

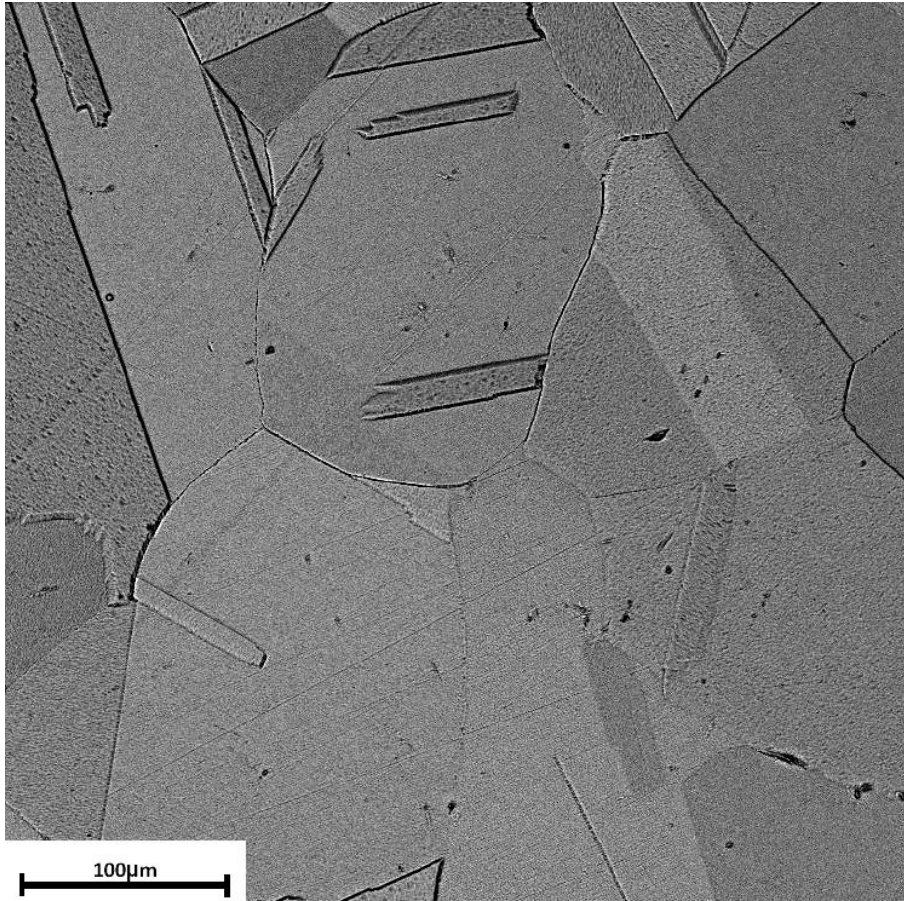


**Fig.2 Microstructure of Cu- 2 wt. % Ti after quenching from 900°C**

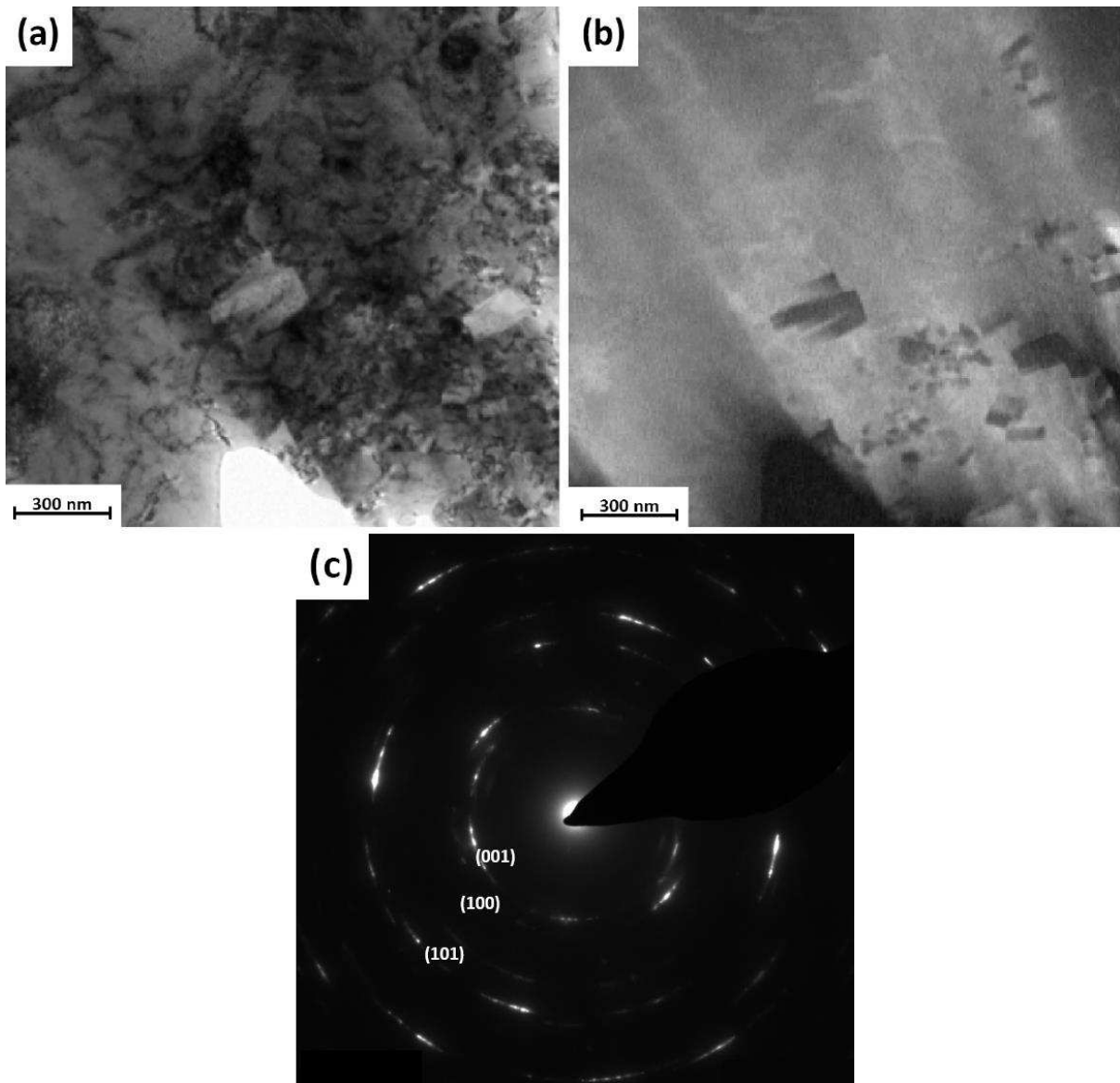


**Fig. 3. a) Bright field TEM image shows tangled dislocations in the vicinity of TiB<sub>2</sub> particles after quenching b) Dark field (c) SAD pattern of TiB<sub>2</sub> particle.**

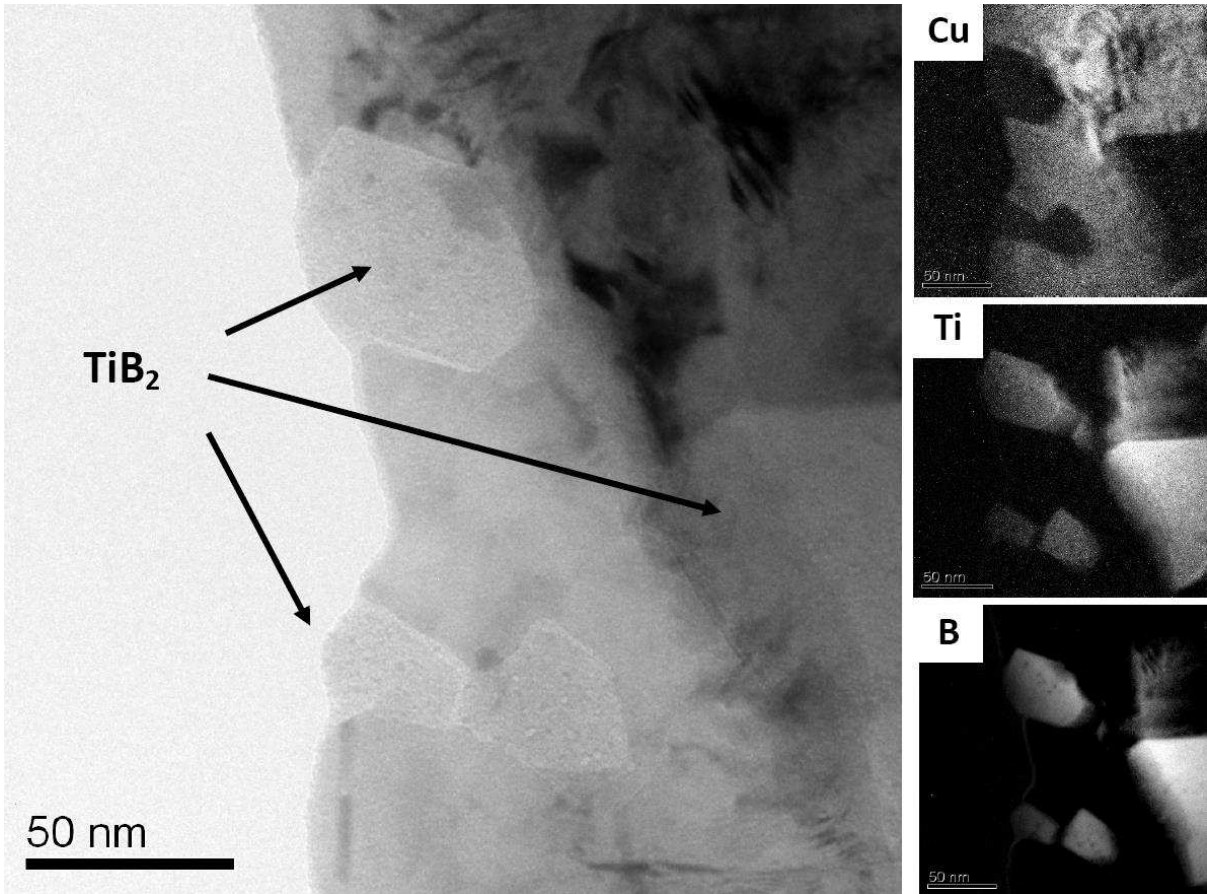


**Fig.4 HRTEM image of the re-solution and quenched Cu-1wt. %Ti-1wt. %TiB<sub>2</sub> with dot point elements maps**

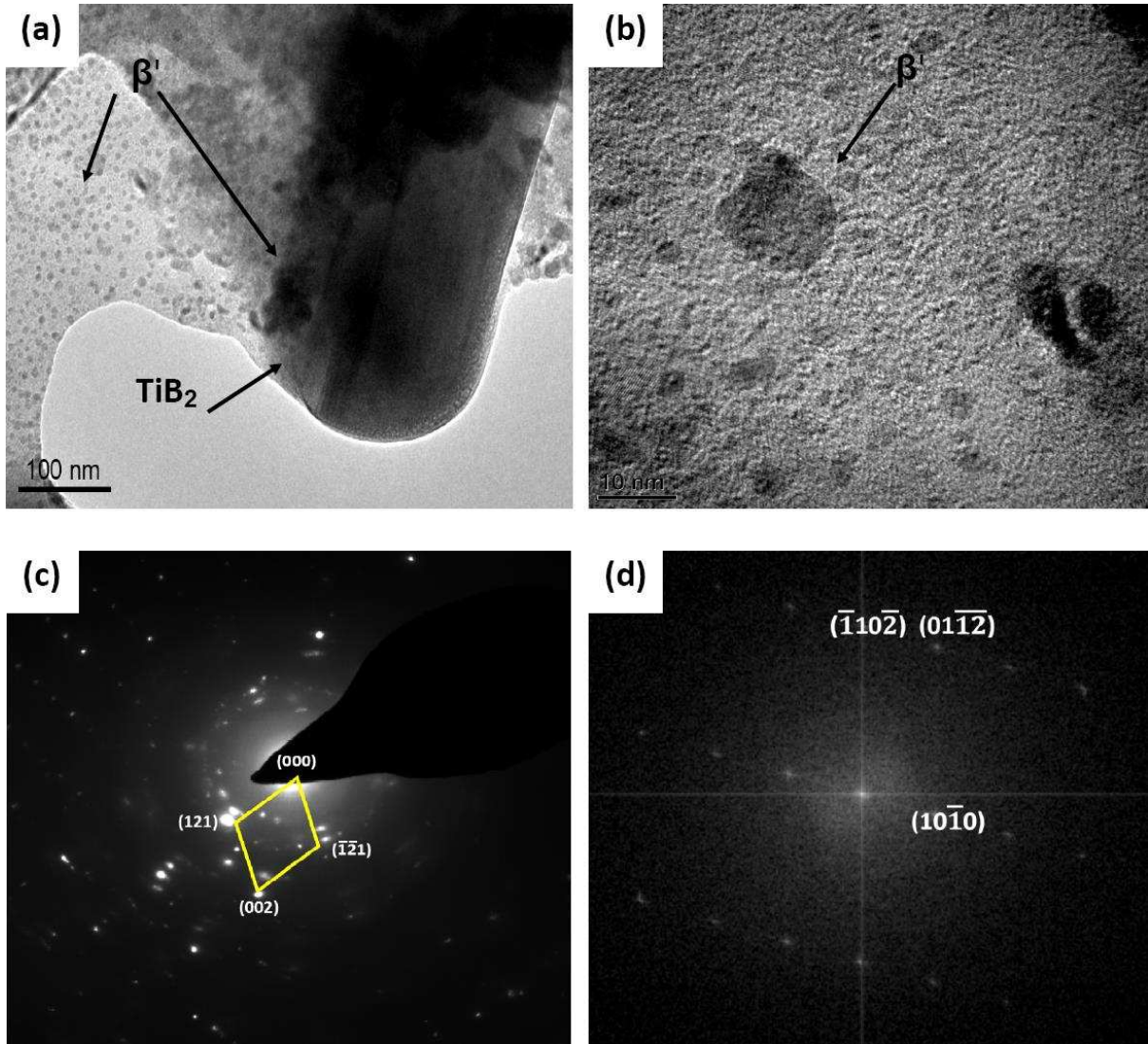


**Fig. 5** HRTEM micrograph of 98 wt.%Cu-1wt. % Ti-1wt. %  $\text{TiB}_2$  aged at 450 °C for 10hrs (a)  $\beta'(\text{Cu}_4\text{Ti})$  formed near the  $\text{TiB}_2$  particle (b)  $\beta'$  growth (c) SAD pattern of  $\beta'(\text{Cu}_4\text{Ti})$  (d)  $\text{TiB}_2$  FFT pattern

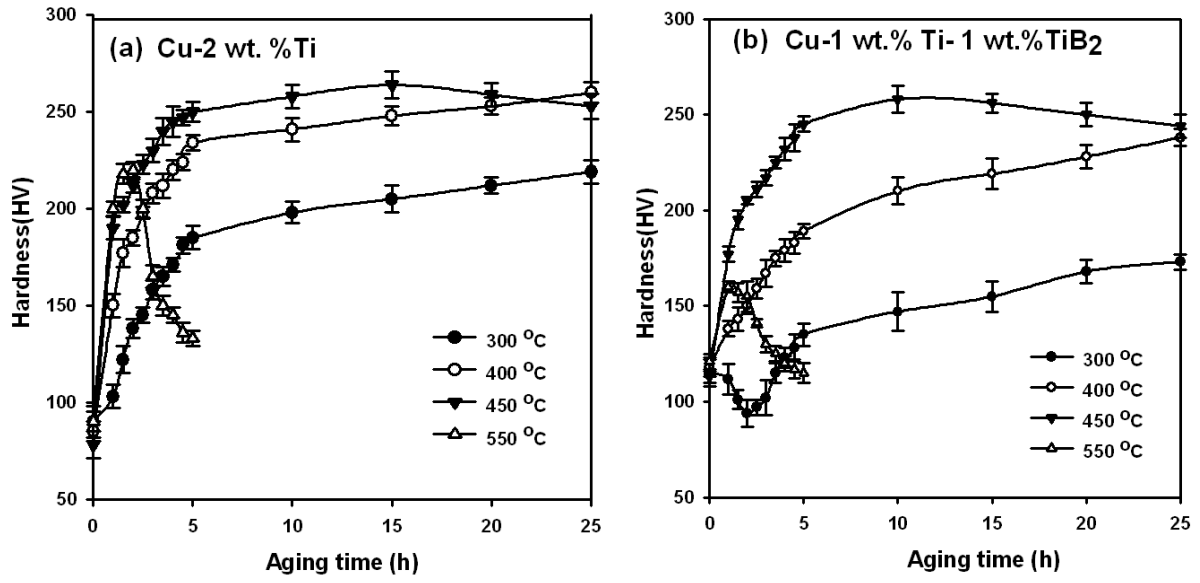
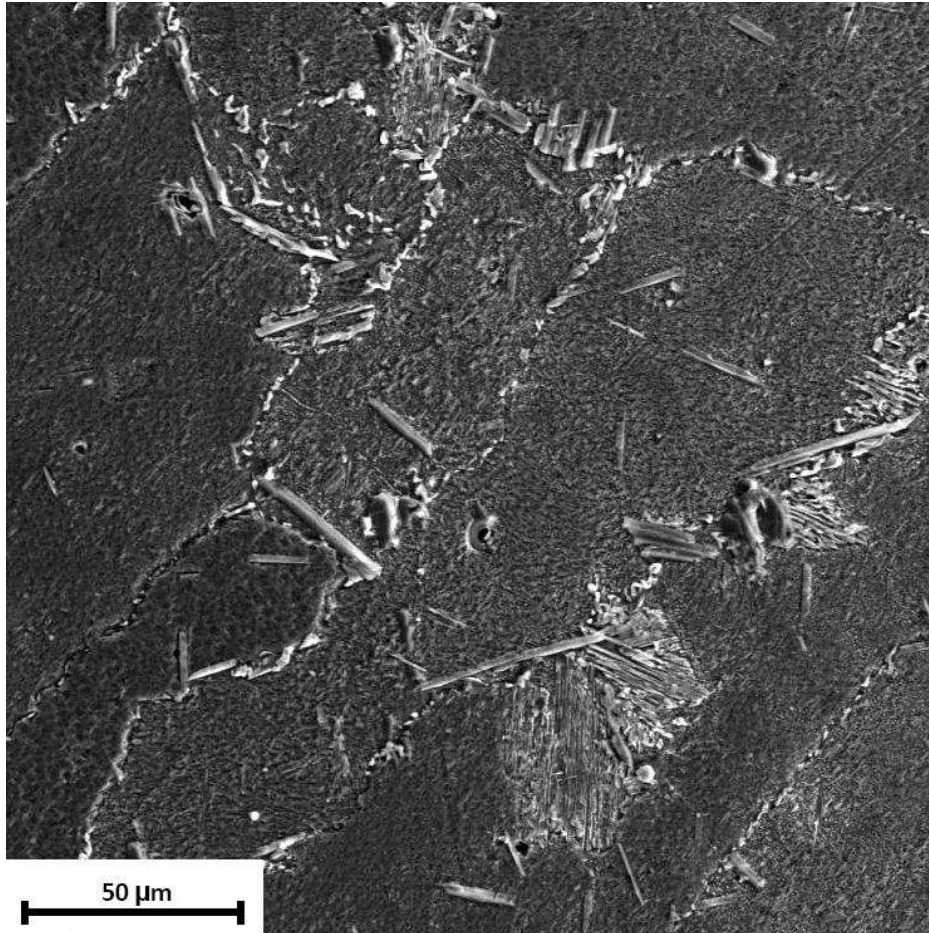
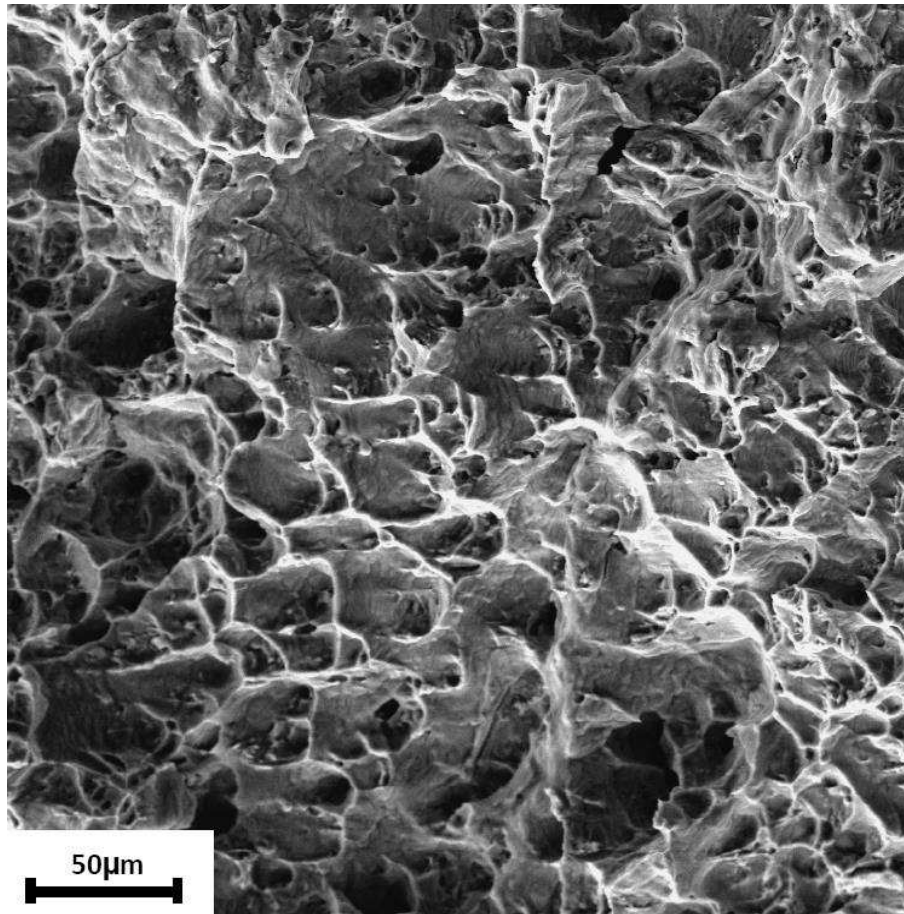


Fig.6. Variation of hardness as a function of ageing time in different temperatures (a) Cu-2 wt. % Ti (b) Cu-1wt. %Ti-1wt. %TiB<sub>2</sub>



**Fig.7. Microstructure of Cu-2 wt. % Ti binary alloy after 25 hrs aged at 450 °C , shows the formation of cellular type precipitate at grain boundaries**



**Fig.8.** Fracture surface of Cu-1 wt. % Ti-1 wt. % TiB<sub>2</sub> composite after 10 hrs aged at 450 °C

**Table.1. Comparison of properties of Cu-1wt. %Ti-1wt. %TiB<sub>2</sub> composite with that for Cu-2 wt. % Ti**

	<u>Cu-1 wt %Ti-1wt% TiB<sub>2</sub></u>			<u>Cu-2 wt% Ti</u>		
	As cast	As quenched	Peak age (10hrs-450°C)	As cast	As quenched	Peak age (15hrs-450°C)
<b>%IACS</b>	8	15	28	7	8	17
<b>Hardness (HV)</b>	85	115	258	115	90	264
<b>YS (MPa)</b>	-	145	415	-	185	417
<b>UTS (MPa)</b>	-	362	590	-	418	615
<b>EI (%)</b>	-	32	21	-	38	24